HENSARD JOURNAL OF ENVIRONMENT

HJ

Article

Geospatial Analysis of Access from Buildings to Health Facilities in Bayelsa, Nigeria.

Academic Editor: Prof. Azizur Rahaman

Received: 15.09.2025
Revised: 15.11.2025
Accepted: 25.11.2025
Published: 04.12.2025

Citation: Islam, Z., Umoru, K., Tobirov, O., & Jabborov, A. (2025). *Geospatial analysis of access from buildings to health facilities in Bayelsa, Nigeria*. **Hensard Journal of Environment**, 1(1).

Zubairul Islam[1], Kebiru Umoru[1,3], Odiljon Tobirov[2]* and A'zamjon Jabborov[2]

[1]Faculty of Environmental Sciences, Hensard University, Toru-Orua, Sagbama Local Government Area, Bayelsa, Nigeria 561001, Nigeria
[2]Department of Geography and Economics, Kokand State University, Kokand, Fergana region, 150700, Uzbekistan.
[3]National Centre for Remote Sensing Jos, Plateau State, Nigeria.
* Correspondence: tobirovodiljon4@gmail.com; Tel.: +998916909200

Abstract

Ensuring timely access to health care in river-delta settings is challenging. This study analyzed geographic accessibility for Bayelsa State, Nigeria at the building level by harmonizing open data in Google Earth Engine to 100 m resolution and estimating least-cost travel time with WHO AccessMod. The cost surface combined Copernicus land cover, OSM roads and waterways, and mode-specific speeds for walking, motorized travel, and boats. AccessMod times were attached to Google Open Buildings footprints, yielding a per-building dataset. We summarized travel time by LGA; screened 5-km hexagons with an impedance ratio (minutes/km) to distinguish near-but-slow barriers from true remoteness; and identified frontier settlement clusters using DBSCAN for TT > 60 min. LGA medians 1–3 min, with Yenegoa, Kolokuma/Opokuma, and Ogbia achieving ≈universal ≤60 min coverage. Long-tail delays align with riverine belts, especially Brass and Ekeremor (e.g., P95 ≈ 65 min). Hex-grid classification across 175,352 buildings shows well-connected 65.7% and typical 29.3%, while actionable problem categories are limited but important: barrier hotspots 1.8%, heterogeneous pockets 1.1%, and remote 0.8% (with 1.4% "No estimate"). Frontier clusters concentrate on the Brass peninsula, the western Ekeremor coast, and scattered southern creek belts (e.g., Odioma-Diema, Cape Formosa, Iduwini wards; median TT typically 62–138 min). Findings indicate that Bayelsa's equity gap is driven less by system-wide distance than by localized impediments. Micro-infrastructure (footbridges, jetties, short feeder links) can resolve near-but-slow hotspots, while outreach/transport support or strategic siting is warranted for truly remote clusters. The reproducible, open-data workflow generalizes to other deltaic contexts.

Keywords: Health Facilities; Accessibility Analysis; GIS.

1. Introduction

Health service accessibility remains a cornerstone of equitable development and public health resilience. Nowhere is this challenge more acute than in Bayelsa State, Nigeria, situated at the heart of the Niger Delta. The state is characterized by an intricate web of rivers, tidal creeks, mangroves, and seasonally inundated floodplains that fragment settlements and constrain mobility. In this riverine environment, the difference between thirty and ninety minutes of travel can determine life or death in obstetric emergencies, severe malaria episodes, or trauma care (Oghenebrume Wariri et al., 2021). While global commitments such as the Sustainable Development Goals emphasize universal health coverage (United Nations, 2015), in practice, households in river-delta ecologies remain systematically disadvantaged by transport delays and fragile infrastructure (Ebener et al.,

2019; Weiss et al., 2015). This enduring structural inequity underscores the urgent need for geographically explicit, context-sensitive studies that extend beyond conventional road-based accessibility modelling (Ray & Ebener, 2008).

Previous research on health access in Nigeria and across sub-Saharan Africa has made important contributions by employing cost-distance surfaces, gridded population data, and facility geocoding to generate national and regional coverage statistics (Dechambenoit, 2016; Kyei-Nimakoh et al., 2017). Such studies have advanced the debate on equity and resource allocation but are limited by their reliance on coarse population rasters, road-dominant friction surfaces, or district-level summaries (Weiss et al., 2018; Alegana et al., 2012). In Bayelsa, the challenge is particularly severe: building-level settlement patterns are fine-grained and discontinuous, and the navigational barriers imposed by water crossings can multiply effective travel times even across short Euclidean distances (Balogun & Onokerhoraye, 2022). Despite the existence of accessibility models, a reproducible, high-resolution, building-resolved analysis that simultaneously quantifies travel time, detects structural barriers, and highlights inequities across local government areas (LGAs) and wards has yet to be undertaken in this context.

This study addresses that gap by introducing a transparent and replicable workflow for spatial accessibility analysis at the building scale. Leveraging Google building footprint data (Google, 2018) enriched with per-building metrics, a calibrated travel-time surface that accounts for waterways and road networks, and geocoded health facility attributes, we construct a multi-layered framework. Our analysis generates outputs that reveal not only how many people are within reach of health facilities but also where hidden inequities and structural barriers persist.

Beyond methodological novelty, the significance of this work lies in its capacity to shift the unit of analysis from coarse administrative averages to the lived geography of buildings and settlements. Conventional accessibility reports often present optimistic coverage statistics, yet these averages conceal stark inequities within LGAs, wards, and even between neighboring villages separated by rivers (Alegana et al., 2018; Ebener et al., 2019). By adopting a building-level lens, we reveal where proximity on a map still translates into delay on the ground. This has immediate practical implications for advancing equity-centered allocation of health services and contributes to a global body of knowledge on health geography in deltaic and floodplain settings.

The specific objectives of this study are to:

1. Quantify building-level time–distance to health facilities and summaries coverage at 30, 60, and 120 minutes.
2. Map 5-km hexagonal impedance hotspots to identify structural barriers where short Euclidean distances belie disproportionately high travel times.
3. Delineate and characterize frontier settlement clusters (>60-minute groups) using density-based clustering, with attributes on dominant LGA, ward, and facility categories.

2. Materials and Methods

2.1 Study area

Bayelsa State lies in the central Niger Delta of southern Nigeria, bounded by Delta State to the west and north, Rivers State to the east, and the Atlantic coastline to the south (Chinda, 2025). Administratively it comprises eight Local Government Areas (LGAs)—Brass, Ekeremor, Kolokuma/Opokuma, Nembe, Ogbia, Sagbama, Southern Ijaw, and Yenagoa (the state capital). The terrain is low-lying and river-dominated, with extensive mangrove and freshwater swamp forests, tidal creeks, and barrier islands. Seasonal flooding and the dense creek network make overland travel circuitous; many settlements are effectively water-dependent, relying on boats for routine mobility (Oyegun et al., 2023). These physical constraints, together with dispersed rural settlements, produce sharp spatial contrasts in access to health facilities: short straight-line distances can translate into long travel times where crossings are absent or road links are discontinuous.

Climatically, Bayelsa experiences a long-wet season and high annual rainfall typical of the deltaic tropics, conditions that further affect road quality and travel speeds, particularly in the outer creek belts (NiMet, 2017). Settlement density and service infrastructure are highest around Yenagoa and the central corridor toward Ogbia/Kolokuma-Opokuma, while the Brass peninsula, western Ekeremor coast, and southern creek margins contain more isolated communities (Onokerhoraye, 2019). For this study, the Bayelsa boundary was taken from FAO-GAUL and all analyses were conducted in EPSG:32632 (WGS 84 / UTM zone 32N) to support metrically consistent distance and travel-time calculations. Figure 1 provides geographic context.

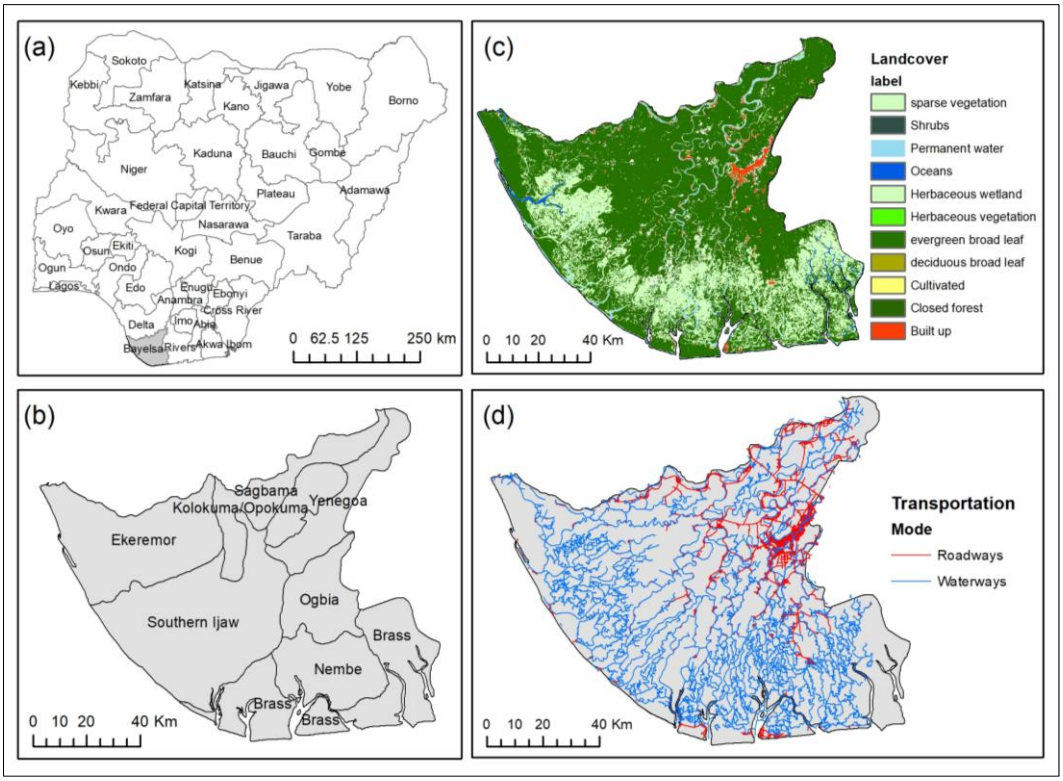

Figure 1. Maps showing the study area in Bayelsa State, Nigeria:
(a) Location of Bayelsa within Nigeria;
(b) Administrative boundaries of Bayelsa State showing Local Government Areas (LGAs);
(c) Land cover classification including vegetation types, wetlands, built-up areas, and water bodies;
(d) Transportation networks, distinguishing roadways (red) and waterways (blue).

2.2 Data collection and harmonization

The datasets were prepared in Google Earth Engine (GEE) and exported at 100 m resolution in EPSG:32632 (WGS 84 / UTM zone 32 N) (Gorelick et al., 2017). The harmonization script (see supplementary) clipped each layer to the FAO GAUL Bayelsa boundary (FAO, 2015) and reprojected continuous variables with bilinear resampling and categorical variables with nearest-neighbor:

- *Elevation & Slope*: SRTM 30 m (USGS, 2014).
- *Land cover*: Copernicus Global Land Cover 100 m (2019) (Buchhorn et al., 2020).
- *Water mask*: JRC Global Surface Water occurrence, thresholded at >50% occurrence (Pekel et al., 2016).
- *Networks*: OpenStreetMap (OSM) roads and waterways were used to define motorized and navigable water routes (Haklay & Weber, 2008).
- *Buildings*: Google building footprints for Bayelsa were accessed in GEE (Google, 2018).

- *Population*: WorldPop 100 m for Nigeria (WorldPop, 2020), reprojected to the 100 m grid; when required for 2024 reporting, population per pixel was temporally projected using a multiplicative growth factor via equation 1.

$$P_{2024}(\mathrm{x}) = P_{2020}(x)(1+r)^{(2024-2020),} \quad (1)$$

where r is a documented annual growth rate (state/national).
All rasters were aligned to the 100 m population grid; all vectors were transformed to EPSG:32632 prior to rasterization or spatial joins.

2.3 Travel-time modelling (AccessMod)

We used WHO AccessMod only to estimate time distance (least-cost travel time to the nearest health facility). AccessMod implements anisotropic least-cost modelling and has been widely applied to equity in health accessibility studies (Ray & Ebener, 2021). The cost surface C (minutes per meter) at cell *i* is the reciprocal of a mode-specific speed v_i (converted to m/min), optionally adjusted for slope if enabled:

$$C_i = \frac{1}{v_i} \times f(slope_i), \quad (2)$$

where f(·) is an anisotropy term (e.g., slope penalty); if disabled, f≡1. Mode and speed assignments followed the study scenario (Table 1), based on established accessibility modelling practices (Ebener et al., 2019).
AccessMod then computes the least-cost accumulated travel time from each cell to the nearest facility using graph-based cost-distance algorithms (Ray & Ebener, 2021).

Table 1 Mode-specific travel speeds (km h^{-1}) for the Bayelsa accessibility model: Motorized for roads, Walking for land cover and Boat for water.

Roads /Motorized		**Land class/Walking**		**Water/Boat**	
Class	(km/h)	Class	(km/h)	Class	(km/h)
Primary	100	Shrubs	4	Permanent water bodies	20
Secondary	80	Herbaceous veg.	5	River	20
Tertiary	50	Cultivated	5	Stream	15
Primary link	90	Built-up	6	Canal	15
Secondary link	60	Sparse vegetation	5	Drain	10
Tertiary link	40	Herbaceous wetland	3		
Unclassified	25	Closed forest	2		
Residential	30	Open forest	3		
Living street	15	Pedestrian	5		
Service	30	Footway	5		
Track	15	Path	4		
Track grade 4	12				
Track grade 5	10				

AccessMod then computes the least-cost accumulated travel time (in minutes) from each cell x to the nearest facility:

$$TT(x) = \min_{\pi \epsilon P(x \to F)} \sum_{(i \to j) \epsilon \pi} C_i \times d_{ij} \quad (3)$$

where π is a path over neighboring cells, d_{ij} is the step length (m), and F is the set of facilities.
The resulting raster was exported and used to populate TT_H per building (nearest-cell sampling).

2.4 Analytical objectives and metrics

All computations used R (R Core Team, 2022) with *sf* (Pebesma, 2018), *dplyr* (Wickham et al., 2023), and *dbscan* (Hahsler et al., 2019) for clustering.

2.4.1 Time–distance to health facilities

Euclidean and travel time distances follow conventions in health accessibility research (Weiss et al., 2020). For each building b, we report the time distance $T_{TH}(b)$ (minutes) and Euclidean distance to the nearest facility $D_{eucl}(b)$ (km), derived from NEAR_DIST (meters):

$$\mathrm{D}_{\mathrm{eucl}}(b) = \max\left(\frac{NEAR\_DIST(b)}{1000}, \in\right), \in = 0.05km \tag{3}$$

Coverage at thresholds $T \in \{30,60,120\}$ min is

$$Cov(T) = \frac{1}{B}\sum_{b=1}^{B} 1\left(TT_H(b) \leq T\right) \times 100\% \tag{4}$$

with B the number of buildings. We also summarize TT_H by median, interquartile range (IQR), and upper tails (p90, p95).

2.4.2 Impedance / barrier hotspots (5-km hex grid)

Our impedance index builds on earlier work that compares travel-time surfaces with straight-line distances to highlight barriers (Makanga et al., 2017). To avoid spurious ratios for co-located features, distances below 50 m were set to 0.05 km. We then overlaid a 5-km hexagonal grid on Bayelsa, joined buildings to hex cells, and summarized each cell with five fields: building count, mean impedance (overall barrier signal), 90th percentile impedance (worst-case conditions), median TT_H, and median Euclidean distance to the nearest facility. For stability, only cells with ≥30 buildings were retained. The resulting layer pinpoints barrier hotspots where targeted measures—bridge improvements, boat services, or feeder-road upgrades—would yield the largest time savings.

2.4.3 Frontier settlement clusters (>60 min)

We identified frontier settlements as dense clusters of buildings whose modeled time to the nearest facility exceeds 60 minutes. Buildings meeting this criterion were reduced to centroids (projected coordinates) and clustered using DBSCAN, treating features as part of the same settlement when they lie within roughly 1.5 km of at least 20 other filtered buildings ($\varepsilon \approx 1.5$ km; minPts = 20). DBSCAN clustering was chosen because it identifies dense groups without requiring the number of clusters a priori (Ester et al., 1996). For each resulting cluster we reported the number of buildings, the median and 90th percentile travel times, and the most common LGA, ward, and nearest-facility category among its members. We also generated a convex-hull polygon and centroid for each cluster and recorded hull area in km² to support operational targeting (e.g., outreach scheduling or siting proposals).

2.5 Software and reproducibility

- Preparation: GEE (Gorelick et al., 2017) with SRTM, Copernicus LC, JRC GSW, WorldPop Nigeria, Bayelsa GAUL boundary; OSM roads/waterways.
- Modelling: WHO AccessMod (Ray & Ebener, 2021).
- Analysis: R (R Core Team, 2022; Pebesma, 2018; Hahsler et al., 2019; Wickham et al., 2023).

3. Results

3.1. Time Distance to Health Facilities

The figure 2 shows a clear core–periphery pattern. Fast access (0–30 min) concentrates in Yenagoa and the central corridor, where dense facilities align with most buildings. Travel times lengthen across the riverine belts and outer LGAs, especially the Brass peninsula and pockets of

Ekeremor/Southern Ijaw, where waterways and sparser road links force detours. Isolated darker patches mark local barriers (e.g., creek crossings) rather than system-wide gaps. This spatial picture matches the box-plots: short medians in every LGA, with a few long-tail cells driving the higher classes seen along coastal and creek-cut edges.

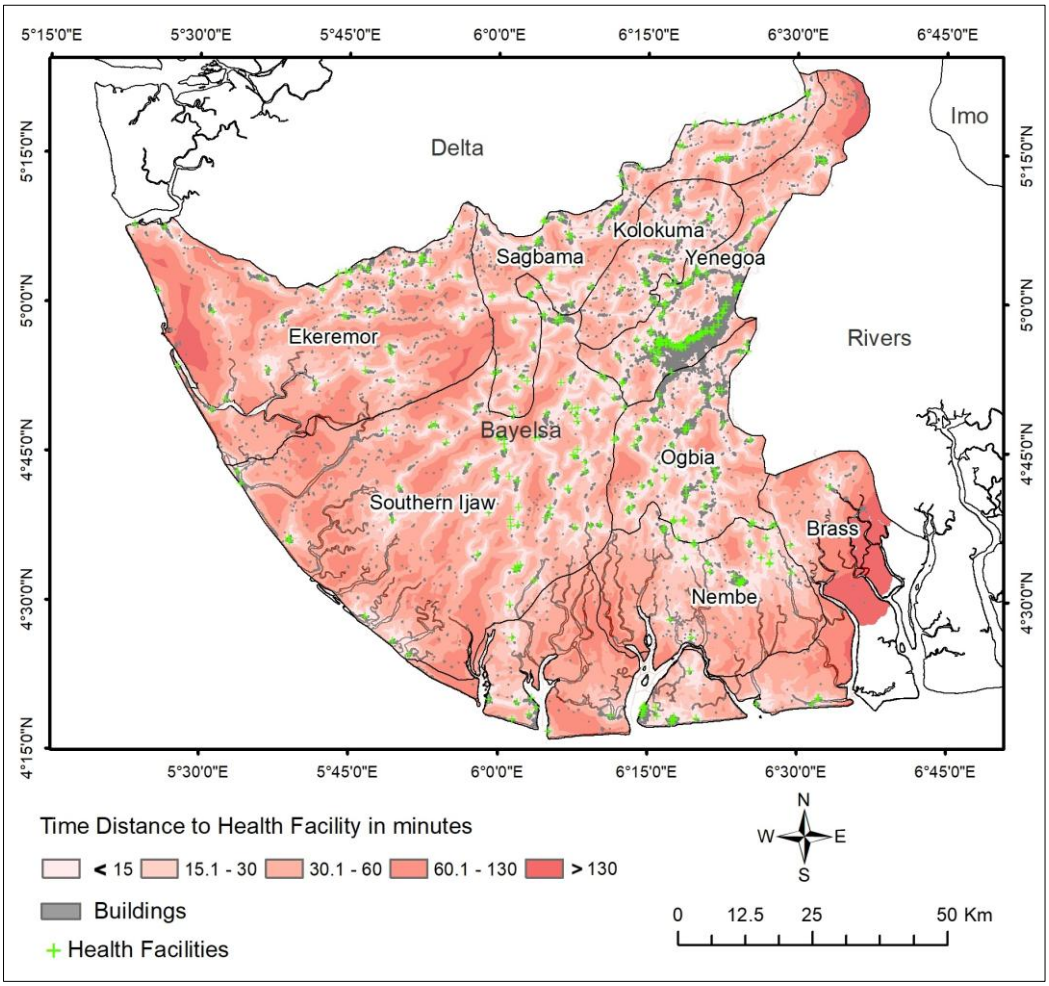

Figure 2. Time-distance to health facilities in Bayelsa State, Nigeria. The map shows spatial accessibility expressed in travel minutes from buildings (grey) to the nearest health facility (green crosses). Accessibility ranges from high (0–15 minutes, light pink) to very low (131–300 minutes, dark red).

Across Bayelsa's LGAs, travel times are bounded right-tails as shown in figure 3. Yenegoa exhibits the strongest performance: a median of 2 minutes (IQR 1), with 100% of buildings within 30, 60, and 120 minutes. Kolokuma/Opokuma and Ogbia show similarly short typical times (both median 2 min, IQR 2) and near-universal coverage: Kolokuma/Opokuma has 99.6% ≤30 min and 100% ≤60/120 min; Ogbia has 99.7% ≤30 min, 99.9% ≤60 min, and 100% ≤120 min.

LGAs with longer upper tails are Brass, Ekeremor, Southern Ijaw, Sagbama, and Nembe. Brass (median 2 min, IQR 6) retains strong coverage (88.1% ≤30 min, 94.5% ≤60 min), but its tail reaches P95 65 min and max 171 min, indicating pockets where residents face substantially longer trips. Ekeremor (median 3 min, IQR 6) shows 87.9% ≤30 min and 93.9% ≤60 min, with a pronounced tail (P90 37 min, P95 65 min, max 191 min). Southern Ijaw (median 2 min, IQR 3) combines 91.9% ≤30 min with very high overall coverage (99.3% ≤60 min, 100% ≤120 min), but still has a notable tail (P90 25 min, P95 37 min). Sagbama (median 2 min, IQR 2) delivers 98.4% ≤30 min and 99.1% ≤60 min, yet reaches P95 17 min and max 199 min, again pointing to localized constraints. Nembe (median 1 min, IQR 2) maintains 92.8% ≤30 min and 97.9% ≤60 min, but the tail extends to P95 40 min and max 94 min.

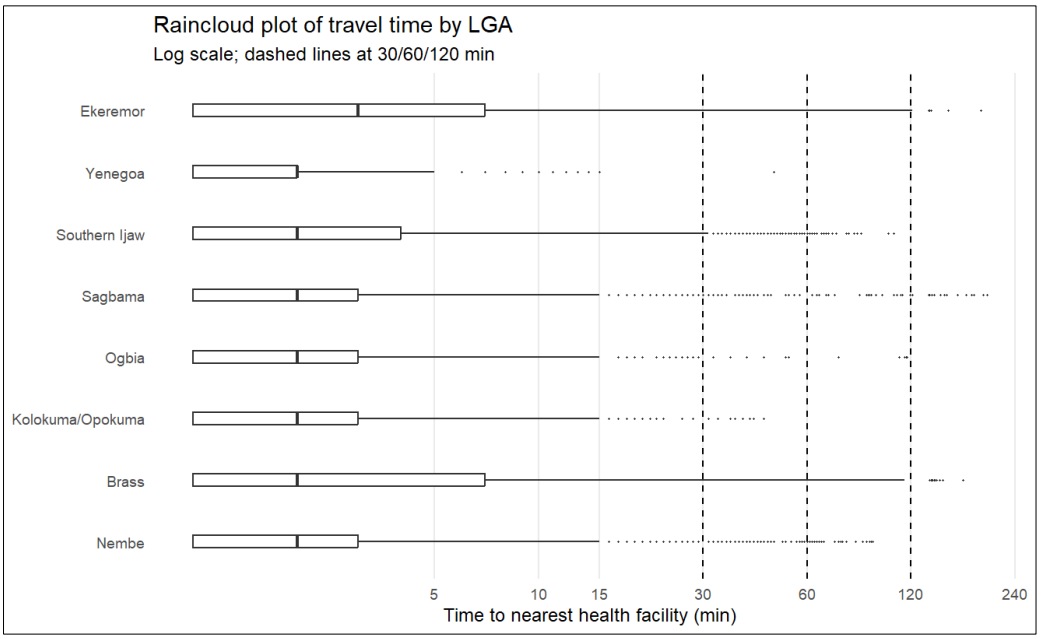

Figure 3. Raincloud/box plots of travel time to the nearest health facility by LGA (log scale). Boxes show median and IQR; dot tails indicate outliers/long delays. Vertical dashed lines mark the 30, 60, and 120-minute thresholds.

3.2. Impedance/Barrier Hotspots (Hex-grid)

We assessed building-level access on a 5-km hexagonal grid and classified each hex using simple, pre-specified rules designed to distinguish good access, structural barriers, and true remoteness. Per-building impedance was calculated as travel time divided by Euclidean distance to the nearest facility, with distances shorter than 0.05 km set to 0.05 km to avoid inflated ratios. For stability, hexes with fewer than 30 buildings were treated as unstable and not used in the calculations. The findings are summarized in Table 2 and shown in Figure 4.

Table 2. Building counts and shares by 5-km hex-grid impedance category in Bayelsa.

Category	**Buildings (n)**	**Share (%)**
Well-connected	115,148	65.7
Typical	51,322	29.3
Barrier hotspot (near but slow)	3,080	1.8
Heterogeneous (pockets of severe delay)	1,933	1.1
Remote (far from care)	1,438	0.8
No estimate	2,431	1.4
Grand Total	175,352	100

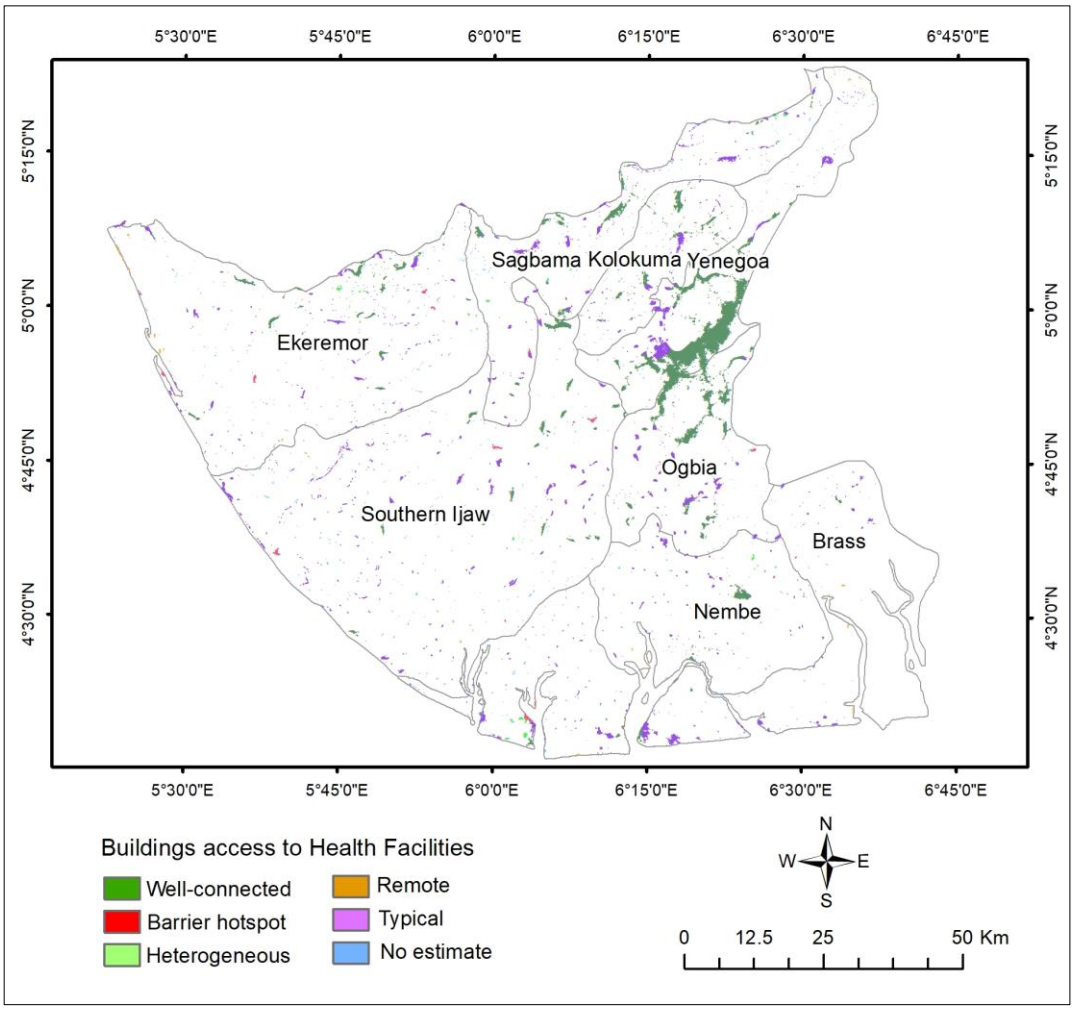

Figure 4. Building-level access classification in Bayelsa (5-km hex–based): well-connected, typical, barrier hotspot (near but slow), heterogeneous pockets, remote, and no estimate (hexes with <30 buildings).

3.2.1 Well-connected

This class comprises 66.6 percent of analyzed buildings, which corresponds to 115,148 buildings. A hex is declared well-connected when the typical travel time is very low (median around ten minutes or less) and the impedance signal is low (on average no more than about five minutes per kilometre). In practical terms, residents in these cells reach care quickly and do not appear to face structural barriers; these areas are baseline/maintenance priorities rather than targets for access expansion.

3.2.2 Typical

This class comprises 29.7 percent of analyzed buildings, which corresponds to 51,322 buildings. A hex is considered typical when it does not trigger any problem flag (i.e., it is neither a hotspot, nor heterogeneous, nor remote under the thresholds below). Access is acceptable on average; these cells provide context for equity but are not the first candidates for intervention.

3.2.3 Barrier hotspots (near but slow)

This class comprises 1.8 percent of analyzed buildings, which corresponds to 3,080 buildings. A hex is labelled a barrier hotspot when buildings are close in straight-line terms—the typical distance to the nearest facility is roughly half a kilometre or less—yet travel remains slow, reflected in high average impedance (about 15 min/km or more) or a high upper tail (the 90th percentile around 20 min/km or more). These patterns usually indicate missing water crossings, circuitous

local links, or seasonal constraints. They are high-leverage opportunities for small, targeted fixes such as footbridges, jetties/ferry points, culverts, or short feeder-road connections.

3.2.4 Heterogeneous pockets (localized severe delays)

This class comprises 1.1 percent of analyzed buildings, which corresponds to 1,933 buildings. A hex is marked heterogeneous when the worst-case impedance is much higher than the average (a pronounced upper tail, with the 90th percentile at least twice the mean and 15 min/km or more). Most residents in these cells fare reasonably well, but specific neighborhoods or links experience severe delay. These places merit micro-targeted interventions at identified bottlenecks.

3.2.5 Remote (far from care)

This class comprises 0.8 percent of analyzed buildings, which corresponds to 1,438 buildings. A hex is labelled remote when typical travel times are long (around 60 minutes or more) and straight-line distances are large (around 3 km or more). These locations are genuinely distant from services and call for transport support, mobile/outreach delivery, or strategic siting or upgrades of facilities.

3.2.6 No estimate (excluded from percentages)

This set contains 2,431 buildings. Hexes appear as "No estimate" when there are no buildings, too few or scattered buildings to meet the stability threshold of 30, or missing inputs for the required metrics. These hexes are shown on maps for completeness but excluded from percentage totals so that results are not biased by unstable or data-poor cells.

3.3 Frontier settlement clusters (>60 min)

Frontier settlements (>60 min). To identify places where many households still face long trips despite generally good statewide access, we clustered buildings with modeled travel time TT > 60 min using DBSCAN (ε≈1.5 km, minPts=20). The resulting frontier clusters represent dense pockets of persistent delay—prime candidates for outreach services, transport support (boats/ambulances), short network links, or, where justified, new facility siting. Clusters concentrate along the Brass peninsula, the western Ekeremor coast, and scattered southern creek belts, with additional pockets in Nembe and Southern Ijaw. Table 3 reports cluster-level size and delay (median and P90 minutes), while Figure 5 maps cluster centroids (red) relative to existing health facilities (green).

Table 3: No. of Buildings and median travel time in Frontier settlement clusters.

LGA	Ward	Buildings (n)	Median TT (min)	P90 TT (min)
Brass	Odioma-Diema	178	138	142
Brass	Cape Formosa	149	71	75
Brass	Odioma-Diema	108	77	78
Brass	Odioma-Diema	63	68	74
Brass	Odioma-Diema	60	106	109
Brass	Minibie	52	86	94.8
Brass	Odioma-Diema	29	63	163.2
Brass	Igbeta Ewoama	22	76	78
Ekeremor	Iduwini 1	324	87	92
Ekeremor	Iduwini 2	219	96	99
Ekeremor	Iduwini 2	114	136	138
Ekeremor	Iduwini 2	83	62	64
Ekeremor	Iduwini 2	57	79	121
Ekeremor	Oyakiri 3	21	103	109

Nembe	Igbeta Ewoama	24	74	75
Nembe	Igbeta Ewoama	22	62	62.9
Southern Ijaw	Iduwini 2	28	64	65
Yenegoa	Asamabiri	61	101	173

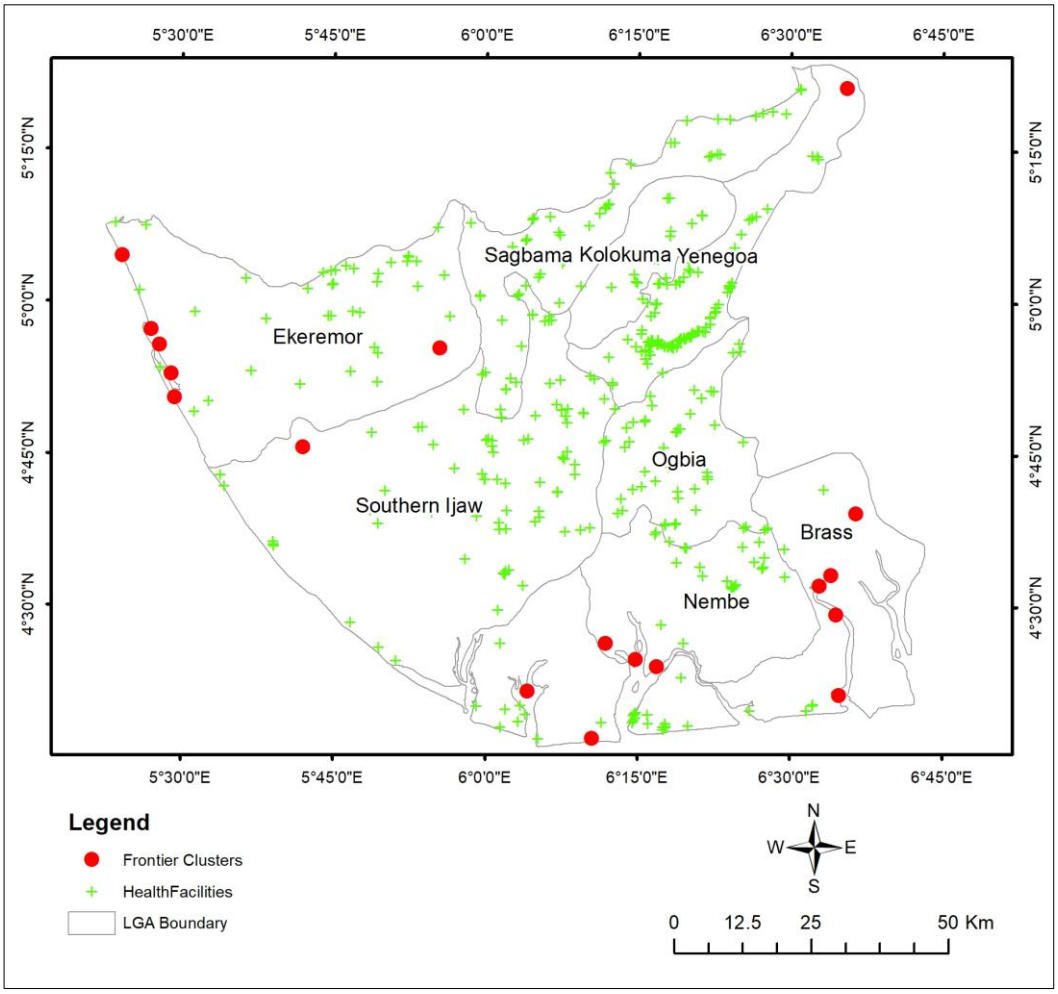

Figure 5. Frontier settlement clusters in Bayelsa. Red circles show cluster centroids where modeled travel time to the nearest health facility exceeds 60 min.

4. Discussion

The present research operates at ≈100 m spatial resolution and produces building-level travel times by attaching the modeled AccessMod time to every Google Open Buildings footprint (via sampling at each building centroid) (Google, 2018; Ray & Ebener, 2021). This lets us diagnose access at the scale where people actually live and move. In contrast, common national/global products at ~1 km resolution are useful for broad inequality assessment but often smooth over settlement-scale barriers within LGAs (Weiss et al., 2018; Weiss et al., 2020). In practical terms, our 100-m workflow can distinguish near-but-slow hotspots (missing crossings, circuitous routes) from true remoteness, something coarse rasters tend to blur. This finer granularity makes the outputs actionable for local governments—supporting micro-infrastructure (bridges, jetties, short feeder links) where impedance is high, and outreach or siting adjustments where distance is the dominant constraint (Makanga et al., 2017).

4.1 Methodological advances over prior studies

First, we harmonized inputs at 100 m in a single CRS and sampled the AccessMod time surface directly to individual buildings (rather than to 1 km pixels or administrative averages), reducing ecological bias and the modifiable areal unit problem. Second, we introduced a hex-grid impedance screen (minutes per kilometre) to separate two mechanisms often conflated in the literature—true remoteness versus near-but-slow barriers—and enforced a ≥30-building stability rule so that sparse cells do not drive results. This complements earlier accessibility studies that report catchment coverage or mean travel time but do not explicitly flag where straight-line proximity fails because of missing crossings or circuitous routes (Ebener et al., 2019). Third, we used DBSCAN clustering on buildings with TT > 60 min to delineate "frontier" settlements without imposing arbitrary shapes—an approach well-suited to fragmented deltaic geographies (Ester et al., 1996).

4.2 Substantive insights relative to prior evidence

Consistent with regional and global studies, we find that waterways and network discontinuities, rather than uniform distance, are the dominant drivers of poor access in riverine settings (Alegana et al., 2012). Our results reproduce the pattern seen in other travel-time work: strong access cores where facilities and roads cluster (Yenagoa, central corridor), and long-tail pockets in peripheral creek networks (e.g., Brass, Ekeremor). What our design adds is the ability to pinpoint micro-locations where residents are "close but slow," a nuance that coarser global or national products cannot consistently reveal (Weiss et al., 2020). The explicit incorporation of surface water occurrence (Pekel et al., 2016) and OSM waterways (Haklay & Weber, 2008) strengthens interpretation of these pockets in Bayelsa's delta landscape.

4.3 Data choices and credibility

We relied on open, peer-reviewed global datasets for population (WorldPop, 2020) and on the evolving Open Buildings inventory for building footprints (Google, 2018). These sources are widely used in accessibility research and humanitarian practice, providing reproducible inputs with clear provenance; our results therefore sit on the same methodological foundations as much of the contemporary literature (Ebener et al., 2019; Ray & Ebener, 2021).

4.4 Policy relevance compared to common approaches

Many studies translate travel time into catchment coverage or 2SFCA-style accessibility scores to guide siting (Luo & Wang, 2003). Our contribution is complementary: by diagnosing mechanism (barrier vs. remoteness) at intervention scale, it yields concrete levers—footbridges/jetties or short feeder links for hotspots; outreach, transport support, or strategic siting for remote clusters—so planners can move beyond "where is far" to "what to fix" and "how". Because the problem categories concern only ~3–4% of buildings while the majority are already well-served, addressing a small set of tails could unlock large equity gains at relatively low cost (Alegana et al., 2018).

4.5 Limitations

As in related work, our speed assumptions are static by mode and cannot capture congestion, tides, seasonality, or facility capacity; several AccessMod studies extend travel time to model capacity-constrained coverage, which could be layered onto our results in future work (Ray & Ebener, 2021; Ebener et al., 2019). OSM networks and Open Buildings may be incomplete in rural creeks (Haklay & Weber, 2008; Google, 2018); WorldPop projections introduce uncertainty at fine scales (WorldPop, 2020). Nonetheless, the concordance between our raincloud/box-plot tails and the mapped riverine barriers, together with stability thresholds and reproducible inputs, suggests that the pattern (who is left behind and where) is robust even if exact minutes vary within plausible speed ranges.

5. Conclusions

This study delivers a high-resolution, building-level picture of geographic access to health facilities in Bayelsa by attaching AccessMod travel times to every Google Open Buildings footprint on a harmonized 100-m grid. The results show a strong baseline: most residents live within short travel times, with well-connected and typical cells accounting for the vast majority of buildings. Yet a small but policy-relevant minority faces actionable constraints: about 3–4% of buildings fall into barrier hotspots or remote/heterogeneous pockets. These long-tail delays cluster along riverine belts and peripheral creek networks—especially parts of Brass and Ekeremor—and are consistent with the raincloud/box-plot evidence (low medians, heavy upper tails).

The practical implication is that Bayelsa's equity gap is not system-wide speed, but localized impediments. Micro-infrastructure (footbridges, jetties, culverts, short feeder links) should be prioritized where impedance is high despite proximity ("near but slow"), while outreach/transport support or strategic siting is warranted for truly remote clusters. Because these pockets are few relative to the whole, targeted action can convert already good averages into consistently fast access for nearly all residents at modest cost.

Methodologically, the work contributes a reproducible, open-data workflow—100-m harmonization, building-level sampling, hex-grid impedance screening with a ≥30-building stability rule, and clustering of >60-minute "frontier" settlements—that can be transferred to other river-delta settings. Key limitations include static speeds, seasonal passability not modelled, and possible network/footprint omissions; nevertheless, the spatial concordance between mapped barriers and statistical tails supports the robustness of the pattern. Future extensions should incorporate seasonality and tides, operational validation (boat/ambulance GPS or travel diaries), and service capacity to link reachability with readiness.

Supplementary Materials: Available at https://github.com/zubairgis/nigeria-hensard

Author Contributions:

Z.I.: Conceptualization, Methodology, Investigation, Formal Analysis, Writing—Original Draft Preparation, Writing—Review and Editing, Visualization.
K.U.: Data Curation, Investigation, Methodology, Writing—Review and Editing.
O.T.: Supervision, Conceptualization, Methodology, Writing—Review and Editing, Project Administration.
A.J.: Validation, Software, Data Curation, Writing—Review and Editing.**Funding:** This research received no external funding.

Data Availability Statement: The satellite data used in this study are open to access as follows:

Administrative: https://developers.google.com/earth-engine/datasets/catalog/ FAO/GAUL/2015/level1
DEM:https://developers.google.com/earth-engine/datasets/catalog/ SGS/SRTMGL1_003
Roads & Water Routes: https://www.openstreetmap.org/#map=6/9.12/8.67
Landcover classes: https://land.copernicus.eu/en/global
Google Building Footprints: https://sites.research.google/gr/open-buildings/

Acknowledgments: The authors are thankful to the Hensard University

Conflicts of Interest: The authors declare no conflicts of interest.

Abbreviations

The following abbreviations are used in this manuscript:

GEE	Google Earth Engine
GIS	Geographic Information System
LULC	Land Use/Land Cover
WHO	World Health Organisation
DEM	Digital Elevation Model

References

Alegana, V. A., Maina, J., Ouma, P. O., Macharia, P. M., Wright, J., Atkinson, P. M., … Tatem, A. J. (2018). National and sub-national variation in patterns of febrile case management in sub-Saharan Africa. *Nature Communications, 9*(1), 4994. https://doi.org/10.1038/s41467-018-07536-9

Alegana, V. A., Wright, J. A., Pentrina, U., Noor, A. M., Snow, R. W., & Atkinson, P. M. (2012). Spatial modelling of healthcare utilisation for treatment of fever in Namibia. *International Journal of Health Geographics, 11*(6), 1–13. https://doi.org/10.1186/1476-072X-11-6

Alegana, V. A., Wright, J. A., Pentrina, U., Noor, A. M., Snow, R. W., & Atkinson, P. M. (2012). Spatial modelling of healthcare utilisation for treatment of fever in Namibia. *International Journal of Health Geographics, 11*(1), 6. https://doi.org/10.1186/1476-072X-11-6

Balogun, V. S., & Onokerhoraye, A. G. (2022). Climate change vulnerability mapping across ecological zones in Delta State, Niger Delta Region of Nigeria. *Climate Services*, *27*, 100304–100304. https://doi.org/10.1016/j.cliser.2022.100304

Buchhorn, M., Lesiv, M., Tsendbazar, N. E., Herold, M., Bertels, L., & Smets, B. (2020). Copernicus Global Land Cover Layers—Collection 2. *Remote Sensing, 12*(6), 1044. https://doi.org/10.3390/rs12061044

Chinda, C.I. (2025). Water Bodies and Economic Development: Perspective on Rivers and Bayelsa States. *Central Asian Journal of Social Sciences and History*, *6*(1), 102–111. https://doi.org/10.17605/cajssh.v6i1.1174

Dechambenoit, G. (2016). Access to health care in sub-Saharan Africa. *Surgical Neurology International*, *7*(1), 108. https://doi.org/10.4103/2152-7806.196631

Ebener, S., Stenberg, K., Brun, M., Monet, J. P., Ray, N., & Hansen, P. (2019). Proposing standardized geographical indicators of physical access to emergency obstetric and newborn care in low-income and middle-income countries. *BMJ Global Health, 4*(5), e000778. https://doi.org/10.1136/bmjgh-2018-000778

Ester, M., Kriegel, H. P., Sander, J., & Xu, X. (1996). A density-based algorithm for discovering clusters in large spatial databases with noise. In *Proceedings of the 2nd International Conference on Knowledge Discovery and Data Mining* (pp. 226–231). AAAI Press.

Ester, M., Kriegel, H. P., Sander, J., & Xu, X. (1996). A density-based algorithm for discovering clusters in large spatial databases with noise. In *Proceedings of the 2nd International Conference on Knowledge Discovery and Data Mining* (pp. 226–231). AAAI Press.

FAO. (2015). *Global Administrative Unit Layers (GAUL): Technical aspects*. Rome: Food and Agriculture Organization of the United Nations.

Google. (2018). *Google Open Buildings Dataset*. Google Research. https://sites.research.google/open-buildings/

Gorelick, N., Hancher, M., Dixon, M., Ilyushchenko, S., Thau, D., & Moore, R. (2017). Google Earth Engine: Planetary-scale geospatial analysis for everyone. *Remote Sensing of Environment, 202*, 18–27. https://doi.org/10.1016/j.rse.2017.06.031

Hahsler, M., Piekenbrock, M., & Doran, D. (2019). dbscan: Fast density-based clustering with R. *Journal of Statistical Software, 91*(1), 1–30. https://doi.org/10.18637/jss.v091.i01

Haklay, M., & Weber, P. (2008). OpenStreetMap: User-generated street maps. *IEEE Pervasive Computing, 7*(4), 12–18. https://doi.org/10.1109/MPRV.2008.80

Kyei-Nimakoh, M., Carolan-Olah, M., & McCann, T. V. (2017). Access barriers to obstetric care at health facilities in sub-Saharan Africa—a systematic review. *Systematic Reviews*, *6*(1). https://doi.org/10.1186/s13643-017-0503-x

Luo, W., & Wang, F. (2003). Measures of spatial accessibility to health care in a GIS environment: Synthesis and a case study in the Chicago region. *Environment and Planning B: Planning and Design, 30*(6), 865–884. https://doi.org/10.1068/b29120

Makanga, P.T., Schuurman, N., Charfudin Sacoor, Boene, H. E., Vilanculo, F., Vidler, M., Magee, L., Dadelszen, P. von, Esperança Sevene, Khátia Munguambe, & Tabassum Firoz. (2017). Seasonal variation in geographical access to maternal health services in regions of southern Mozambique. *International Journal of Health Geographics*, *16*(1). https://doi.org/10.1186/s12942-016-0074-4

NiMet (Nigerian Meteorological Agency). (2017). *Climate review bulletin: 2016–2017 season*. Abuja: NiMet Publications.

Oghenebrume Wariri, Egwu Onuwabuchi, Albin, J., Dase, E., Iliya Jalo, Laima, C. H., Halima Usman Farouk, El-Nafaty, A. U., Uduak Okomo, & Dotse-Gborgbortsi, W. (2021). The influence of travel time to health facilities on stillbirths: A geospatial case-control analysis of facility-based data in Gombe, Nigeria. *PLoS ONE*, *16*(1), e0245297–e0245297. https://doi.org/10.1371/journal.pone.0245297

Onokerhoraye, A. G. (2019). The geography of healthcare delivery in the Niger Delta. *Benin Journal of Social Sciences, 27*(2), 14–32.

Oyegun, C. U., Lawal, O., & Ogoro, M. (2023). The Niger Delta Region. *World Geomorphological Landscapes*, 107–121. https://doi.org/10.1007/978-3-031-17972-3_7

Pebesma, E. (2018). Simple features for R: Standardized support for spatial vector data. *The R Journal, 10*(1), 439–446. https://doi.org/10.32614/RJ-2018-009

Pekel, J. F., Cottam, A., Gorelick, N., & Belward, A. S. (2016). High-resolution mapping of global surface water and its long-term changes. *Nature, 540*(7633), 418–422. https://doi.org/10.1038/nature20584

R Core Team. (2022). *R: A language and environment for statistical computing*. Vienna: R Foundation for Statistical Computing. https://www.R-project.org/

Ray, N., & Ebener, S. (2008). AccessMod 3.0: computing geographic coverage and accessibility to health care services using anisotropic movement of patients. *International Journal of Health Geographics*, *7*(1), 63–63. https://doi.org/10.1186/1476-072x-7-63

United Nations. (2015). *Transforming our world: The 2030 Agenda for Sustainable Development*. United Nations General Assembly. https://sdgs.un.org/2030agenda

USGS. (2014). *SRTM 1 Arc-Second Global (SRTMGL1)* [Data set]. United States Geological Survey. https://doi.org/10.5066/F7PR7TFT

Weiss, D. J., Nelson, A., Gibson, H. S., Temperley, W., Peedell, S., Lieber, A., … Tatem, A. J. (2018). A global map of travel time to cities to assess inequalities in accessibility in 2015. *Nature, 553*(7688), 333–336. https://doi.org/10.1038/nature25181

Weiss, D. J., Nelson, A., Vargas-Ruiz, C. A., Gligoric, K., Bavadekar, S., Gabrilovich, E., … Tatem, A. J. (2020). Global maps of travel time to healthcare facilities. *Nature Medicine, 26*(12), 1835–1838. https://doi.org/10.1038/s41591-020-1059-1

Wickham, H., François, R., Henry, L., Müller, K., & Vaughan, D. (2023). *dplyr: A grammar of data manipulation* (R package version 1.1.4). https://CRAN.R-project.org/package=dplyr

WorldPop. (2020). *WorldPop Global High Resolution Population Datasets* [Data set]. WorldPop, University of Southampton. https://www.worldpop.org/